

*This paper reports an analytical solution to one of the problems related to applied mechanics and acoustics, which tackles the analysis of free axisymmetric bending oscillations of a circular plate of variable thickness. A plate rigidly-fixed along the contour has been considered, whose thickness changes by parabola  $h(\rho)=H_0(1+\mu\rho)^2$ . For the initial assessment of the effect exerted by coefficient  $\mu$  on the results, the solutions at  $\mu=0$  and some  $\mu\neq 0$  have been investigated. The differential equation of the shapes of a variable-thickness plate's natural oscillations, set by the  $h(\rho)$  function, has been solved by a combination of factorization and symmetry methods. First, a problem on the oscillations of a rigidly-fixed plate of the constant thickness ( $\mu=0$ ), in which  $h(1)/h(0)=\eta=1$ , was solved. The result was the computed natural frequencies (numbers  $\lambda_i$  at  $i=1\dots 6$ ), the constructed oscillation shapes, as well as the determined coordinates of the nodes and antinodes of oscillations. Next, a problem was considered about the oscillations of a variable-thickness plate at  $\eta=2$ , which corresponds to  $\mu=0.4142$ . Owing to the symmetry method, an analytical solution and a frequency equation for  $\eta=2$  were obtained when the contour is rigidly clamped. Similarly to  $\eta=1$ , the natural frequencies were calculated, the oscillation shapes were constructed, and the coordinates of nodes and antinodes of oscillations were determined. Mutual comparison of frequencies (numbers  $\lambda_i$ ) shows that the natural frequencies at  $\eta=2$  for  $i=1\dots 6$  increase significantly by (28...19.9) % compared to the case when  $\eta=1$ . The increase in frequencies is a consequence of the increase in the bending rigidity of the plate at  $\eta=2$  because, in this case, the thickness in the center of both plates remains unchanged, and is equal to  $h=H_0$ . The reported graphic dependences of oscillation shapes make it possible to compare visually patterns in the distribution of nodes and antinodes for cases when  $\eta=1$  and  $\eta=2$ . Using the estimation formulae derived from known ratios enabled the construction of the normalized diagrams of the radial  $\sigma_r$  and tangential  $\sigma_\theta$  normal stresses at  $\eta=1$  and  $\eta=2$ . Mutual comparison of stresses based on the magnitude and distribution character has been performed. Specifically, there was noted a more favorable distribution of radial stresses at  $\eta=2$  in terms of strength and an increase in technical resource*

*Keywords: natural frequencies, oscillation shapes, analytical solution, circular plate, free oscillations, symmetry method*

UDC 534.8  
DOI: 10.15587/1729-4061.2020.201073

# ANALYTICAL SOLUTION TO THE PROBLEM ABOUT FREE OSCILLATIONS OF A RIGIDLY CLAMPED CIRCULAR PLATE OF VARIABLE THICKNESS

**K. Trapezon**

PhD, Associate Professor  
Department of Acoustic and Multimedia Systems  
National Technical University of Ukraine "Igor Sikorsky Kyiv Polytechnic Institute"  
Peremohy ave., 37, Kyiv, Ukraine, 03056  
E-mail: kirill.trapezon@gmail.com

**A. Trapezon**

Doctor of Technical Sciences, Leading Research  
Laboratory No. 7.1  
G. S. Pisarenko Institute for Problems of Strength  
of the National Academy of Sciences of Ukraine  
Timiryazevs'ka str., 2, Kyiv, Ukraine, 01014  
E-mail: trapezon@ukr.net

Received date 22.04.2020

Accepted date 09.07.2020

Published date 27.08.2020

Copyright © 2020, K. Trapezon, A. Trapezon

This is an open access article under the CC BY license

(<http://creativecommons.org/licenses/by/4.0>)

## 1. Introduction

Plates of different outlines and thicknesses are widely used in modern technical devices as structural elements operating in variable mode. In this regard, one should note the frequently mentioned elements related to construction sites, instrumentation and engineering structures, aerospace units. These elements include building floors, foundation slabs, the bottoms of tanks and pistons in the internal combustion engines, as well as aircraft empennage components. Examples of the latest applications include wind turbines [1], turbojet engines, and navigation water vessels [2]. In the latter case, specific plate devices are used to increase the ship's velocity, which control the resistance of the water environment [2]. Issues concerning the important scope of application, relevance, and practical demand for the results from studying and calculating plate oscillations are addressed in many literary sources, for example, in [3–7]. Earlier, paper [8] outlined the essence of the problem and gave a brief overview of how to solve it, as regards round plates of vari-

able thickness. It is noted, in particular, that the problem of the oscillations of solid plates of variable thickness remains unresolved. At best, calculating the oscillations of such plates employs numerical methods for determining their natural frequencies. The relevance of the task to calculate the oscillations of a solid plate of variable thickness is due to the practical demand for plate elements. Therefore, it is an actual issue to develop an estimation model, which would produce an analytical solution to the eigenvalue problem, suitable for the subsequent calculation of frequencies and the construction of shapes of natural oscillations. In addition, there is also the possibility to determine the cyclical stresses that occur in the plate when it is deformed.

## 2. Literature review and problem statement

Our analysis of current publications [1, 2, 9–15] leads to the conclusion that solving the problem about bending oscillations of circular plates is in high demand for research-

ers and specialists in applied acoustics and mechanics. This judgment is supported by the presence of a huge number of technical applications of circular plates and various ways to solve the relevant eigenvalue problem. However, most of the methods and algorithms considered in [1, 2, 9–15] are specific and focus on iterative numerical approaches. In addition, the results reported in the cited papers typically refer to plates of constant thickness. As regards plates of variable thickness with a parabolic profile, no mathematical apparatus has been found for the analytical calculation of bending oscillations.

In work [9], an analysis of oscillations for bending and shear deformation of the continuous thickness circular plate was carried out on the basis of the numerical iterative method of dynamic softening in combination with a finite difference method. In essence, judging by the above calculations, expressions for calculating displacements and stresses are artificial since they are tied to solving a “numerical” code based on an iterative method. However, the given recommendations cannot be used in the analysis of the curved oscillations of a variable-thickness plate.

In paper [10], the authors emphasize the need for accurate analysis of circular elastic plates. Cylindrical coordinates are used to represent expressions for calculating natural frequencies and shapes of oscillations, but only for plates of constant thickness based on Mindlin’s theory. However, it is not possible to adapt the reported results for variable-thickness plates, given the lack of an appropriate mathematical apparatus in the cited paper.

Article [11] examines the physical basis for the propagation of curved edge waves over the surface of a thin circular plate. The authors separately investigated the effect exerted by the values of the Poisson coefficient on the wave shapes observed at the surface of the plate. An analysis of the article reveals that the object of the authors’ research is only a plate of constant thickness. The results reported in the article are not applicable to the problem of bending oscillations of a variable-thickness plate.

Work [12] considers a ceramic circular plate of the constant thickness ( $h=1$  cm), exposed to thermal loads at the surface. A simplex method is recommended to analyze the dynamic thermal bend of the plate. Under conditions of temperature deformation, expressions were obtained to calculate oscillation shapes, their natural frequencies were determined. However, it follows from the formulated statement of the problem that those expressions concern not the plate but the thermal membrane. Therefore, it is not advisable to use the results reported in the work for a solid plate of variable thickness under normal temperature regimes.

In articles [12, 13], the object of the study is a circular metallic-ceramic plate of constant thickness, which is subject to increased temperature loads. However, in contrast to work [12], it is suggested to use a free grid method of interpolation for a bend analysis. Under conditions of considering the surface temperature of the plate (from 20 °C to 200 °C) and the associated change in the thickness of the plate, the reported theory and results are not possible to use for the analysis of free axisymmetric oscillations of a continuous circular plate of parabolic profile.

Based on four analytical functions and a generalized “English” method, work [14] provides a solution to the equation of the shapes of a plate’s natural oscillations. However, when the problem is examined in detail, it turns out that the plate of constant thickness is under the influence of the transverse load  $p(r, \theta)$ . In a given statement of the problem, a force in the

radial direction is expressed through the Fourier series using a biharmonic function. Therefore, the results derived on the basis of a 3D analytical solution under a biharmonic load cannot be applied for the problem of free bending oscillations for a plate with a parabolic profile of thickness change. In addition, the proposed “English” method is based on a 3D theory of elasticity and implies that the coefficient of a plate’s material (Poisson coefficient) can arbitrarily change along the radial profile of the plate. This feature also imposes restrictions on the solution to the problem of a solid plate of variable thickness.

In article [15], the authors considered a plate with variable thickness, stiffness, and density using the parameter  $p$ . However, it should be noted that the authors artificially create in their study a function of changing the  $E$  elasticity module, density  $\rho$ , thickness  $h$  along the radius of the plate:  $E=E_0(1+p(r/R)^2)^{n+0.5}$ ;  $\rho=\rho_0(1+p(r/R)^2)^{n-0.5}$ ;  $h=h_0(1+p(r/R)^2)^{0.5}$ . These parameters are selected in such a way that they correspond to the original equation of the oscillation shapes. In this case, this equation is easily solved by traditional methods. If one accepts  $p=0$ , one obtains a problem for a plate of constant thickness. As a result, we are dealing with an artificial approach and therefore conclude that there is no progress towards solving a problem of calculating plates of variable thickness.

Thus, a review of the above literature allows us to conclude that there are no publications addressing the analytical solution to the problem of bending free oscillations of a circular plate of a parabolic profile. The reason, of course, is not the lack of interest in the possibility of solving the problem but apparently is the difficulties of a mathematical nature, in the absence of a correct solution method. The works cited above [14, 15] are indicative in this respect. These studies apply a “new approach” to achieve the goals stated, the essence of which is to treat absolutely arbitrarily the elastic and physical constants of a material, considering these constants to be variables. Paper [14] introduces a “material’s coefficient”, variable along the radius of the plate, instead of the Poisson coefficient. Work [15] introduced the elasticity module  $E(r)$  and the density  $\rho(r)$ , variable along the radius. As a result of this “method”, work [15], for example, “converts” the constant thickness of the plate into a variable and a simple problem turns into a problem about the oscillations of a plate of variable thickness. Our analysis suggests that it is appropriate to conduct a study on the construction of an analytical solution to the problem of free oscillations of a circular plate of the parabolic profile. In this case, it would be possible to expand the range of profiles of solid plates of variable thickness, which are subject to calculation within the framework of Kirchhoff’s theory. In turn, as the review suggests, this has scientific and applied importance.

---

### 3. The aim and objectives of the study

---

The aim of this study is to analytically solve the eigenvalue problem using an example of examining free axisymmetric oscillations of a rigidly fixed circular plate. The thickness of the plate varies according to the parabolic law  $h(\rho)=H_0(1+\mu\rho)^2$ . For the initial assessment of the effect exerted by  $\mu$  on the results, it is advisable to consider solutions at  $\mu=0$  and some  $\mu\neq 0$ .

To accomplish the aim, the following tasks have been set:  
– it is required to use the factorization method in order to move from the original differential equation of the fourth

order for a plate of the predefined thickness to a system of two equations of the second order;

- to solve the problem about a plate’s oscillations at  $\mu=0$ , which corresponds to  $\eta=h(1)/h(0)=1$ , by determining the natural frequencies, cyclical deflections, as well as the coordinates of nodes and antinodes of oscillations;

- to solve a similar problem using the symmetry method at  $\mu\neq 0$ , by selecting  $\mu=0.4142$ , which corresponds to  $\eta=2$ . Compare the results of the calculation of oscillations at  $\eta=1$  and  $\eta=2$ ;

- to construct diagrams of the radial and tangential normal stresses, which occur during the cyclical deformation of plates of constant ( $\eta=1$ ) and variable ( $\eta=2$ ) thickness. Compare the results by establishing the impact exerted by the parameter  $\mu$  on them.

---

#### 4. The original differential equation and its transformation

---

A differential equation of the shapes of a circular plate’s natural axisymmetric oscillations with the thickness that changes according to the law  $h=H_0H(\rho)$  is obtained if one separates the time multiplier  $\cos(\omega t)$  in a known equation, given, for example, in work [8]. As a result, this equation for the deflections  $W(\rho)$  can be written in the form

$$W^{(4)} + 2 \frac{(\rho H^3)'}{\rho H^3} W''' + \left[ \frac{(H^3)''}{H^3} + \frac{(H^{6+3\nu})'}{H^{6+3\nu}} \right] W'' + \frac{1}{\rho H^3} \left[ \nu (H^3)' - \frac{H^3}{\rho} \right] W' - \frac{\lambda^4}{H^2} W = 0, \tag{1}$$

where

$$\lambda^2 = \frac{\omega R^2}{H_0} \sqrt{\frac{12(1-\nu^2)\gamma}{gE}}; \tag{2}$$

$\rho=r/R$ ;  $r, R$  is the relative, variable, and constant radii;  $H(\rho), H_0$  is the variable and constant of thickness;  $\omega=2\pi f, f$  are the circular and linear frequencies;  $\nu, E, \gamma$  is the Poisson coefficient, the elasticity module, and the specific weight of a material;  $g$  is the acceleration of gravity.

We accept the value of the Poisson coefficient to be  $1/3$ , which is acceptable for most structural metallic materials. Under the law  $h=H_0(1+\mu\rho)^2$ , equation (1) can be rewritten in a symbolic form:

$$\left( H \frac{d^2}{d\rho^2} + \frac{(H^2\rho)'}{H\rho} \frac{d}{d\rho} - 2\mu^2 \right)^2 W - (\lambda^4 + 4\mu^4) W = 0. \tag{3}$$

Such a representation, in accordance with the factorization method, makes it possible to replace the equation of the fourth order (3) with two equations of the second order

$$HW'' + \frac{(H^2\rho)'}{H\rho} W' - 2\mu^2 W \pm \sqrt{\lambda^4 + 4\mu^4} W = 0. \tag{4}$$

In this case, a general solution to equation (3) will be derived as the sum of the solutions to these two equations, that is,  $W=W_1+W_2$ , where  $W_1$  is the solution to equation (4) at a plus sign before the square root, and  $W_2$  – at a minus sign.

Once we introduce expression  $H=(1+\mu\rho)^2$  to (4), we obtain

$$W'' + \frac{[\rho(1+\mu\rho)^4]'}{\rho(1+\mu\rho)^4} W' + \frac{k_*^2}{(1+\mu\rho)^2} W = 0, \tag{5}$$

where

$$k_*^2 = -2\mu^2 \pm \sqrt{\lambda^4 + 4\mu^4} = \mu^2 \left[ -2 \pm \sqrt{(\lambda/\mu)^4 + 4} \right].$$

Equations (5) cannot be analytically solved at  $\mu\neq 0$ ; however, solutions to such equations can be built using the symmetry method [16].

In accordance with the purpose of the current work, and for the sake of certainty, we further consider two types of plates of thickness  $h=H_0(1+\mu\rho)^2$ : at  $\mu=0$  ( $h=H_0=\text{const}$ ) and at  $\eta=2$ , where  $\eta=h(\rho=1)/h(\rho=0)$  is the ratio of the thickness on the contour  $h(1)=H_0(1+\mu)^2$  to the thickness in the center of the plate  $h(0)=H_0$ . For the case  $\eta=2$ , we obtain  $\mu=0.4142$ .

---

#### 5. Solving the problem for a plate of constant thickness, rigidly fixed along the contour

---

At  $\mu=0$ , we obtain  $h=H_0$ , and, in this case, equations (5) take the form of Bessel equations

$$W'' + \frac{W'}{\rho} \pm \lambda^2 W = 0.$$

Solutions to these equations, written in a detailed form

$$W_1'' + \frac{W_1'}{\rho} + \lambda^2 W_1 = 0, \quad W_2'' + \frac{W_2'}{\rho} - \lambda^2 W_2 = 0, \tag{6}$$

produce, in sum, a solution for deflections (oscillation shapes) in the form

$$W = W_1 + W_2 = AJ_0(\lambda\rho) + BI_0(\lambda\rho) = A \left[ J_0(\lambda\rho) + \frac{B}{A} I_0(\lambda\rho) \right], \tag{7}$$

where  $A, B$  are the constants of the integration, dependent on boundary conditions.

When the contour is rigidly fixed ( $\rho=1$ ), the boundary conditions take the form

$$(W)_{\rho=1} = 0; \quad (W_\rho)_{\rho=1} = 0. \tag{8}$$

After introducing (7) to (8), we obtain two equations

$$\begin{cases} AJ_0(\lambda) + BI_0(\lambda) = 0, \\ AJ_1(\lambda) - BI_1(\lambda) = 0, \end{cases}$$

based on which it is possible to determine the relationship of amplitude coefficients

$$\frac{B}{A} = \frac{J_1(\lambda)}{I_1(\lambda)} = -\frac{J_0(\lambda)}{I_0(\lambda)}, \tag{9}$$

and to obtain an equation of frequencies

$$J_0(\lambda) / I_0(\lambda) + J_1(\lambda) / I_1(\lambda) = 0. \tag{10}$$

The results of the calculation of oscillations of a rigidly clamped plate of constant thickness are given in Table 1.

**Table 1**  
The results of oscillation calculation at  $\eta=1$

$\eta$	$\lambda_i$	$B/A_i$	Oscillation node coordinates $\rho_{0i}$	Oscillation antinode coordinates $\rho_{mi}$
1	3.19622	0.05571	1	0
			0.379	0
	6.306437	-0.00253	1	0.616
			0.255	0
	9.439499	0.00011	0.583	0.406
			1	0.782
			0.191	0
	12.57713	$-4.83096 \cdot 10^{-6}$	0.439	0.305
			0.687	0.59
			1	0.812
			0.153	0
	15.716438	$2.09655 \cdot 10^{-7}$	0.351	0.244
			0.551	0.456
			0.749	0.64
			1	0.85
18.856545	$-9.08545 \cdot 10^{-9}$	0.128	0	
		0.293	0.203	
		0.459	0.391	
		0.625	0.542	
		0.791	0.71	
1	0.88			

The deflections, that is, the oscillation shapes for the first three eigen numbers  $\lambda_1, \lambda_2, \lambda_3$  (Table 1), are shown in Fig. 1 by graphical dependences.

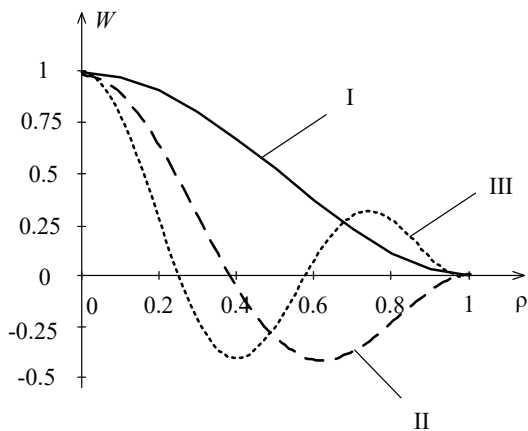


**Fig. 1.** Graphic image of deflections on the first three oscillation shapes

Fig. 1 and Table 1 provide complete information about the parameters of a freely oscillating rigidly clamped plate of constant thickness.

**6. Solving the problem for a variable-thickness plate by symmetry method**

Transform equations (5) by replacing the variable  $\rho = \rho(x)$  to the form, that is, expressed through the variable  $x(\rho)$

$$W_{xx} + \frac{F_x}{F} W_x + k^2 W = 0. \tag{11}$$

Assuming  $x = \ln(1 + \mu\rho)$ , find

$$F(x) = D^2(x) = e^{4x} - e^{3x}; k^2 = \left[ -2 \pm \sqrt{\left(\frac{\lambda}{\mu}\right)^4 + 4} \right]. \tag{12}$$

A solution to equation (11) at  $D^2(x) = e^{4x} - e^{3x}$  is unknown, so  $D(x)$  needs to be approximated by such  $D_1(x)$  function at which such a solution is possible. Because, as noted in chapter 4, at the plate's thicknesses ratio  $\eta = h(1)/h(0) = 2$ ,  $\mu = 0.4142$  was obtained, then, in this case, according to the dependence  $x = \ln(1 + \mu\rho)$ , the limits  $\rho = 0 \div 1$  are matched with the limits to the new variable  $x = 0 \div \ln 2 / 2 = 0 \div 0.347$ .

For a given interval  $x$ , we shall choose the following expression as an approximating function

$$D_1 = D_{01} \sqrt{x} I_0(nx), \tag{13}$$

where  $D_{01} = 1.1; n = 4.64$ .

The plot of function (13) within the required interval is shown in Fig. 2. Fig. 2 also shows, for comparison, the graphic image of the original function  $D(x)$ .

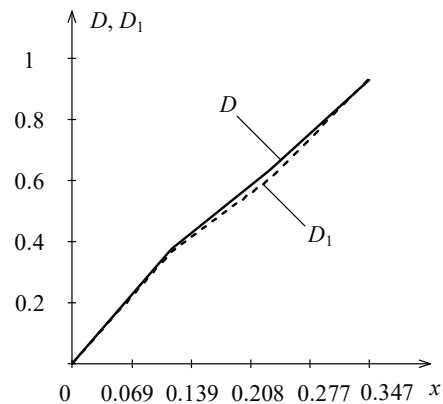


**Fig. 2.** Graphic image of approximation functions

Equations (11) for function (13) will be written in the form

$$\begin{aligned} W_1'' + 2 \frac{D_1'}{D_1} W_1' + \alpha^2 W_1 &= 0; \\ W_2'' + 2 \frac{D_1'}{D_1} W_2' - \beta^2 W_2 &= 0, \end{aligned} \tag{14}$$

where

$$\alpha^2 = \sqrt{\left(\frac{\lambda}{\mu}\right)^4 + 4} - (2 + n^2);$$

$$\beta^2 = \sqrt{\left(\frac{\lambda}{\mu}\right)^4 + 4} + (2 + n^2). \tag{15}$$

The exact solutions to equations (14), obtained by the symmetry method, are

$$W_1 = \frac{AJ_0(\alpha x) + BY_0(\alpha x)}{I_0(nx)};$$

$$W_2 = \frac{A_1I_0(\beta x) + B_1K_0(\beta x)}{I_0(nx)}. \tag{16}$$

The overall solution  $W$  to the original equation of the fourth order is the sum of the solutions  $W_1$  and  $W_2$ . Given that  $Y_0(\alpha x)$  and  $K_0(\beta x)$  at  $x=0$  tend to infinity, these functions, in order to ensure the resulting deflections in the center of the plate (at  $x=0$ ), need to be excluded from solutions (16), adopting the coefficients  $B=B_1=0$ . The overall solution to equation (3), expressed through the variable  $x$ , should be written in the form

$$W = \frac{AJ_0(\alpha x) + A_1I_0(\beta x)}{I_0(nx)} = \frac{A_1}{I_0(nx)} \left[ \frac{A}{A_1} J_0(\alpha x) + I_0(\beta x) \right]. \tag{17}$$

If a plate is rigidly clamped along the contour  $\rho=1$  ( $x=x_1 = \ln 2/2$ ), then it is necessary to meet the conditions

$$(W)_{x=x_1} = 0;$$

$$(x_\rho W_x)_{x=x_1} = (W_x)_{x=x_1} = 0. \tag{18}$$

After introducing function (17) and its derivative to (18), we obtain a frequency equation

$$\alpha \frac{J_1(\alpha x_1)}{J_0(\alpha x_1)} + \beta \frac{I_1(\beta x_1)}{I_0(\beta x_1)} = 0, \tag{19}$$

and equivalent ratios to calculate the amplitude coefficients

$$\frac{A}{A_1} = - \frac{I_0(\beta x_1)}{J_0(\alpha x_1)} = \frac{\beta I_1(\beta x_1)}{\alpha J_1(\alpha x_1)}. \tag{20}$$

The roots of frequency equation (19) for the first six eigenvalues of the problem are given in Table 2.

The character of change in deflections, that is, the form of oscillation shapes, for the first three eigenfrequencies  $\lambda_1 \div \lambda_3$  (Table 2), is illustrated by the graphic dependences shown in Fig. 3.

Fig. 3 and Table 2 provide a clear pattern of the free oscillations of a circular rigidly clamped plate of variable thickness.

Table 2

Results of oscillation calculation at  $\eta=2$

$\eta$	$\alpha_i$	$\beta_i$	$\lambda_i$	$A/A_{1i}$	Oscillation node coordinates $\rho_{0i}$	Oscillation antinode coordinates $\rho_{mi}$
2	8.9389853	10.841	4.11502	31.47856	1	0
	18.1179444	19.128	7.71665	545.59803	0.341	0
					1	0.561
	27.2008023	27.884	11.40923	11273.20989	0.222	0
					0.54	0.36
	36.26957009	36.785	15.13035	$-2.45681 \cdot 10^5$	1	0.755
					0.165	0
	45.3349641	45.748	18.86406	$5.47859 \cdot 10^6$	0.396	0.267
					0.649	0.54
	54.39937355	54.744	22.60442	$-1.23637 \cdot 10^8$	1	0.812
					0.131	0
	45.3349641	45.748	18.86406	$5.47859 \cdot 10^6$	0.313	0.212
0.508					0.388	
54.39937355	54.744	22.60442	$-1.23637 \cdot 10^8$	0.717	0.576	
				1	0.828	
54.39937355	54.744	22.60442	$-1.23637 \cdot 10^8$	0.109	0	
				0.257	0.175	
54.39937355	54.744	22.60442	$-1.23637 \cdot 10^8$	0.416	0.354	
				0.585	0.537	
54.39937355	54.744	22.60442	$-1.23637 \cdot 10^8$	0.761	0.745	
				1	0.838	

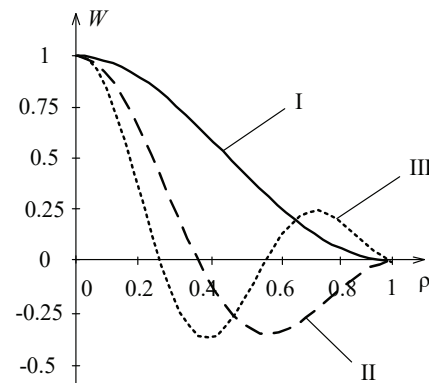


Fig. 3. Graphic image of deflections on the first three oscillation shapes

### 7. Stresses at oscillations of a rigidly clamped circular plate

To analyze the stressed-strained state of a circular plate at axisymmetric bending or axisymmetric oscillations, we shall use known ratios to calculate the radial  $\sigma_r$  and tangential  $\sigma_\theta$  normal stresses, maximal for thickness.

$$\sigma_r = -\frac{6D}{h^2} \left( W_{rr} + \frac{\nu}{r} W_r \right); \quad \sigma_\theta = -\frac{6D}{h^2} \left( \nu W_{rr} + \frac{1}{r} W_r \right). \tag{21}$$

Here,  $W_r, W_{rr}$  are the derivatives for radius  $r=0 \div R$ , where  $R$  is the radius of a plate;  $D = Eh^3/12(1-\nu^2)$  is the cylindrical rigidity.

After the transition to the relative variable  $\rho=r/R$ , adopting  $\nu=1/3, h=H_0$ , and omitting a minus sign due to

the stress cyclic nature, expression (21) can be rewritten in a modified form.

$$\begin{cases} \sigma_r = \frac{9}{16} \frac{EH_0}{R^2} \left( W_{\rho\rho} + \frac{1}{3\rho} W_\rho \right); \\ \sigma_\theta = \frac{9}{16} \frac{EH_0}{R^2} \left( \frac{1}{3} W_{\rho\rho} + \frac{1}{\rho} W_\rho \right). \end{cases} \quad (22)$$

If a plate has a constant thickness  $h=H_0$ , then, according to (6), we obtain

$$W_{\rho\rho} = (W_2 - W_1)\lambda^2 - \frac{W_\rho}{\rho},$$

where

$$W_\rho = \lambda \left[ -AJ_1(\lambda\rho) + BI_1(\lambda\rho) \right].$$

Using these expressions and omitting the intermediate mathematical calculations, we shall obtain the estimation formulae from (22)

$$\begin{cases} \sigma_r = \sigma_0 \lambda^2 A \left\{ \frac{2}{3\lambda\rho} J_1(\lambda\rho) - J_0(\lambda\rho) + \frac{B}{A} \left[ -\frac{2}{3\lambda\rho} I_1(\lambda\rho) + I_0(\lambda\rho) \right] \right\}; \\ \sigma_\theta = \sigma_0 \frac{\lambda^2}{3} A \left\{ -\frac{2}{\lambda\rho} J_1(\lambda\rho) - J_0(\lambda\rho) + \frac{B}{A} \left[ \frac{2}{\lambda\rho} I_1(\lambda\rho) + I_0(\lambda\rho) \right] \right\}; \end{cases} \quad (23)$$

where  $\sigma_0 = (9EH_0)/(16R^2)$ ;  $B/A$  corresponds to dependences (9). Note that since it follows from the recurrent formulae for the Bessel functions that

$$\lim_{\lambda\rho \rightarrow 0} \left[ \frac{J_1(\lambda\rho)}{\lambda\rho} \right] = \frac{1}{2}; \quad \lim_{\lambda\rho \rightarrow 0} \left[ \frac{I_1(\lambda\rho)}{\lambda\rho} \right] = \frac{1}{2},$$

then, for  $\sigma_r$  and  $\sigma_\theta$  at  $\rho=0$ , we shall obtain the resulting values, that is,

$$\sigma_r(0) = \sigma_\theta(0) = \sigma_0 \lambda^2 A \frac{2}{3} \left( \frac{B}{A} - 1 \right).$$

If one accepts  $\sigma_r(0) = \sigma_\theta(0) = 1$ , then  $A = 3/2\sigma_0\lambda^2(B/A - 1)$ . With the help of (23) and data from Table 1, we built diagrams of the radial and tangential cyclical stresses (Fig. 4) for the main shape of oscillations of a circular plate of constant thickness with a rigid attachment of the contour.

For a plate of the variable thickness  $h = H_0(1 + \mu\rho)^2$ , at the thickness ratios  $\eta = 2$  and  $\mu = 0.4142$ , we derived the solutions to (17), expressed through the variable  $x = \ln(1 + \mu\rho)$ . It is advisable therefore to rewrite ratios (21) depending on a given variable  $x(\rho)$ .

After the necessary transformations, we shall obtain

$$\begin{cases} \sigma_r = \sigma_0 (W_{xx} + PW_x); \\ \sigma_\theta = \frac{\sigma_0}{3} (W_{xx} + qW_x); \end{cases} \quad (24)$$

where

$$\sigma_0 = \frac{9}{16} \frac{H_0 E}{R^2} \mu^2; \quad P = \frac{e^x}{3(e^x - 1)} - 1; \quad q = \frac{3e^x}{e^x - 1} - 1.$$

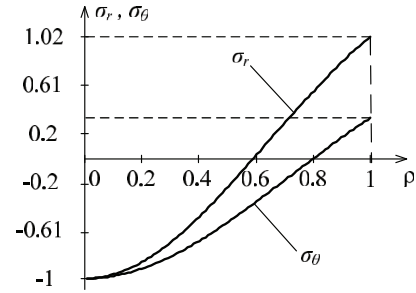


Fig. 4. Graphic image of the radial and tangential normal stresses  $\sigma_r, \sigma_\theta$  at the first shape of oscillations, if  $\eta=1$

For the convenience of subsequent calculations, let us express  $W_{xx}$  through  $W_x$  and  $W = W_1 + W_2$  by using equations (14) and the solutions to (17). We obtain

$$W_{xx} = -2 \frac{D_1'}{D_1} W_x + \beta^2 W_2 - \alpha^2 W_1,$$

where

$$W_x = \left[ \frac{AJ_0(\alpha x) + A_1 I_0(\beta x)}{I_0(\alpha x)} \right]_x;$$

$$W_1 = A \frac{J_0(\alpha x)}{I_0(\alpha x)};$$

$$W_2 = A_1 \frac{I_0(\beta x)}{I_0(\beta x)}.$$

In the end, we shall obtain the estimation formulae from (24)

$$\begin{cases} \sigma_r = \frac{\sigma_0}{I_0(\alpha x)} \left\{ -A \left[ M \cdot S + \alpha^2 J_0(\alpha x) \right] + \right\}; \\ \sigma_\theta = \frac{\sigma_0}{3I_0(\alpha x)} \left\{ -A \left[ L \cdot S + \alpha^2 J_0(\alpha x) \right] + \right\}; \end{cases} \quad (25)$$

where

$$M = \frac{e^x}{3(e^x - 1)} - \left[ 1 + \frac{1}{x} + 2n \frac{I_1(\alpha x)}{I_0(\alpha x)} \right];$$

$$L = \frac{3e^x}{e^x - 1} - \left[ 1 + \frac{1}{x} + 2n \frac{I_1(\alpha x)}{I_0(\alpha x)} \right];$$

$$S = \alpha J_1(\alpha x) + n \frac{I_1(\alpha x)}{I_0(\alpha x)} J_0(\alpha x);$$

$$U = \beta I_1(\beta x) - n \frac{I_1(\beta x)}{I_0(\beta x)} I_0(\beta x).$$

With the help of formulae (25), after the transition to the variable  $\rho = r/R$ , we built diagrams of the radial and

tangential cyclical stresses (Fig. 5) for the main shape of oscillations of a solid plate of variable thickness with a rigid attachment of the contour.

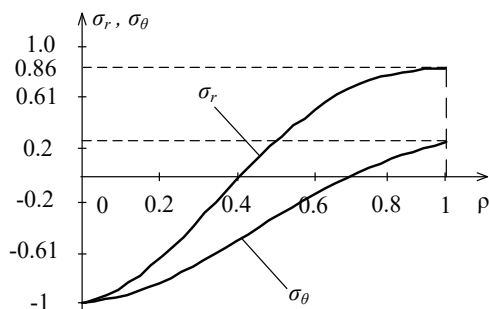


Fig. 5. Graphic image of the radial and tangential normal stresses  $\sigma_r, \sigma_\theta$  at the first shape of oscillations, if  $\eta=2$

Fig. 4, 5 show the differences in the distribution of stresses  $\sigma_r$  and  $\sigma_\theta$ , arising in the plates of constant and variable thickness when oscillating in the first shape.

### 8. Discussion of results of solving a problem for a solid variable-thickness plate

The fourth-order equation (1) cannot be solved under an arbitrary law of change in the thickness of a plate  $h(\rho)$ . The current paper shows that the considered case for the thickness  $h=H_0(1+\mu\rho)^2$  makes it possible to apply a factorization method to this equation. According to this method, the desired function  $W(\rho)$  is represented as the sum of the solutions to two second-order equations (5). This is an important result because the second-order equations are in any case easier to solve than a fourth-order equation at least by the series method. It is clear from the analysis of these equations that the possibility to solve them analytically is limited only to the case  $\mu=0$ . In order to establish patterns of changes in the characteristics of oscillations depending on the relative thickness of the plate  $\eta=h(1)/h(0)$ , which is in turn dependent on the parameter  $\mu$ , it is necessary to solve the problem for a series of different values of  $\mu$ . As an example, to compare such characteristics, the current paper has considered two cases, at  $\mu=0$  ( $\eta=1$ ) and  $\mu=0.4142$  ( $\eta=2$ ).

First, the problem was solved about the oscillations of a rigidly clamped plate of the constant thickness ( $\mu=0; \eta=1$ ). The result was the calculated eigen numbers  $\lambda_i$  ( $i=1...6$ ), the constructed oscillation shapes for  $\lambda_i$  ( $i=1,2,3$ ), and the determined coordinates of the nodes and antinodes of oscillations. To compare the variants of the solutions, we next considered the problem of a variable-thickness plate's oscillations at  $\eta=2$ , which corresponds to  $\mu=0.4142$ . The symmetry method was used to solve equations at a given  $\mu \neq 0$ . According to the method, replacing the variable coefficient  $D(x)$  with the equivalent function  $D_1(x)$  over the required interval (Fig. 2) makes it possible to derive an exact solution to equations (5). It should be noted that because of the flexibility of the symmetry method, there are no rigid restrictions to select the  $D_1(x)$  function. It can be expressed, for example, not only through the Bessel functions [18]. It is owing to the method of symmetry that an analytical solution and a frequency equation for  $\eta=2$  were obtained when the plate is rigidly clamped. Similarly

to  $\eta=1$ , we calculated the eigen numbers  $\lambda_i$  ( $i=1...6$ ), built the oscillation shapes for  $\lambda_i$  ( $i=1,2,3$ ), and determined the coordinates for the nodes and antinodes of oscillations.

Based on the calculation of the oscillations for cases  $\eta=1$  and  $\eta=2$ , given in Tables 1, 2, and shown in Fig. 1, 2, one can note the following. The mutual comparison of frequencies (numbers  $\lambda_i$ ) shows that the natural frequencies at  $\eta=2$  for  $i=1...6$  increase significantly compared to the case of  $\eta=1$ , starting at 28% ( $i=1$ ) and gradually falling to 19.9% ( $i=6$ ). The increase in the natural frequencies is a consequence of the increased rigidity for bending the plate at  $\eta=2$ , given that in this case the thickness in the center of both plates remains unchanged and is equal to  $h=H_0$ . When comparing the oscillation shapes (Fig. 1, 3), one can see their similarity but the coordinates of the oscillation nodes (at  $i>1$ ), given in the tables and visible in the figures indicate their quantitative difference. It consists, as one can see, of the differences in the length of the gaps between the nodes, respectively, at  $\eta=1$  and  $\eta=2$ . The shorter this gap at the equal values of  $W(\rho)$ , the greater the curvature of this function, and the greater, therefore, the curved radial stresses  $\sigma_r$  in the antinode between these nodes. One can see that the gaps between the nodes at  $\eta=2$  are smaller than those at  $\eta=1$ , which is why one should expect such stresses to exceed, at  $\eta=2$ , the stresses at  $\eta=1$ . In addition to the above general considerations regarding the stresses, we analyzed the plate's stressed state at  $\eta=1$  and  $\eta=2$  for the principal shape of oscillations. Using the estimation formulae derived from known ratios, we built the normalized diagrams of the radial  $\sigma_r$  and tangential  $\sigma_\theta$  cyclic stresses (Fig. 4, 5). The mutual comparison of the  $\sigma_r, \sigma_\theta$  values at  $\rho=0$  and  $\rho=1$  shows the following.

There is an inequality  $\sigma_r(1)/\sigma_r(0) > 1$  in the plate of the constant thickness ( $\eta=1$ ). In this case, the ratio is 1.02. If a plate is axisymmetrically thickened from the center to the clamped contour ( $\rho=1$ ), the ratio  $\sigma_r(1)/\sigma_r(0)$  decreases, in particular, at  $\eta=2$  (Fig. 5), it is 0.86. Since the main effect on the strength of the plate elements is exerted by  $\sigma_r$ , which is known from the experiments reported in [19, 20], controlling the value of  $\sigma_r(1)/\sigma_r(0)$  by changing  $\eta$  is of practical importance. First, the possibility of a reasonable reduction of this value makes it possible to successfully study the strength of materials at the ratio of the principal stresses of  $\sigma_r(1)/\sigma_r(0)=1$ , because the destructive stresses would occur in the center. Comparing the course of the curves for  $\sigma_r$  in Fig. 5 for  $\eta=2$  shows that, in comparison with Fig. 4, for  $\eta=1$  there is a smoother change in  $\sigma_r$ , the area adjacent to the attachment. This indicates a more favorable distribution of stresses in the case of  $\eta=2$  because, in terms of strength, a danger zone, which is the attachment, is no longer sharply concentrated along the edge, as is the case for  $\eta=1$ . Therefore, such a plate is more rational in terms of reliability and technical resource.

The procedure considered to solve the problem about the axisymmetric natural oscillations of a parabolic-profile plate with a rigid attachment imposes special conditions for the choice of the parameter  $\eta$ . A change in the magnitude of  $\eta$  may require a change in the approximation function (13). However, given the flexibility of the symmetry method, this procedure is feasible.

Further advancement of the current study may relate to a change in the boundary conditions along the contour of the plate and to extending the range for the parameter  $\eta \neq 1$ , which determines the concaveness of the plate.

## 9. Conclusions

1. Through the factorization method, the original differential equation of the fourth order for the oscillation shapes of a variable-thickness circular plate has been reduced to a system of two second-order equations. The thickness of the plate changes according to the parabolic law  $h(\rho) = H_0(1 + \mu\rho)^2$ . This intermediate result is crucial because, given the limited capabilities of the noted method, it cannot be implemented for any thickness  $h(\rho)$ .

2. A problem about the oscillations of a rigidly fixed plate at  $\mu=0$ , which corresponds to  $\eta=h(1)/h(0)$ , has been solved. We have computed the eigen numbers  $\lambda_i$  ( $i=1\dots6$ ), built the oscillation shapes for  $\lambda_i$  ( $i=1\dots3$ ), and gave the coordinates of the nodes and antinodes of displacements.

3. A similar problem has been solved at  $\mu \neq 0$  for the case of  $\eta=2$ . We have computed and determined the oscillation parameters, similar to the case of  $\eta=1$ . The method of symmetry has been used to produce reliable results in an analytical form since, after the proper approximation of variable coefficients in the equations of the second order, a solution is obtained in a closed form. The oscillations parameters,

established at  $\eta=1$  and  $\eta=2$ , were compared. It was found, in particular, that the natural frequencies  $\lambda_i$  at  $\eta=2$  for  $i=1\dots6$  essentially, by (28...19.9) %, increase compared to the case of  $\eta=1$ . It was noted that this increase is associated with an increase in the curved stiffness of the plate at  $\eta=2$  compared to the stiffness at  $\eta=1$  because the thickness at  $\rho=0$  remains unchanged. We also performed a mutual comparison of the coordinates of nodes and antinodes of oscillations.

4. Based on our calculations, the diagrams of the radial  $\sigma_r$  and tangential  $\sigma_\theta$  normal stresses arising in the plate at axisymmetric oscillations on the principal shape have been built. A comparative analysis of the stressed state of the plate at  $\eta=1$  and  $\eta=2$  was performed. For a plate of the constant thickness ( $\eta=1$ ), it has been established that  $\sigma_r(1)/\sigma_r(0)=1.02>1$ ; for a plate of variable thickness at  $\eta=2$ , this ratio is  $0.86<1$ . Since, as we established, the main effect on the strength of round plates is exerted by the radial stresses  $\sigma_r$ , controlling the value of  $\sigma_r(1)/\sigma_r(0)$  by changing  $\eta$  is of practical importance, for example, when testing materials for durability. There are also some qualitative differences in the course of the  $\sigma_r$  and  $\sigma_\theta$  curves, respectively, at  $\eta=1$  and  $\eta=2$ , which can affect operational reliability and technical resource.

## References

1. Kulkarni, P., Dhoble, A., Padole, P. (2018). A review of research and recent trends in analysis of composite plates. *Sādhanā*, 43 (6). doi: <https://doi.org/10.1007/s12046-018-0867-1>
2. Cucinotta, F., Nigrelli, V., Sfravara, F. (2017). Numerical prediction of ventilated planing flat plates for the design of Air Cavity Ships. *International Journal on Interactive Design and Manufacturing (IJIDeM)*, 12 (2), 537–548. doi: <https://doi.org/10.1007/s12008-017-0396-x>
3. Leissa, A. W. (1969). *Vibration of Plates*. NASA SP-160. United States, 362.
4. Panovko, Ya. G. (1967). *Osnovy prikladnoy teorii uprugih kolebaniy*. Moscow: Mashinostroenie, 316.
5. Bitseno, K. B., Grammel', R. (1952). *Tekhnicheskaya dinamika*. Vol. II. Moscow: GITTL, 638.
6. Kovalenko, A. D. (1959). *Kruglye plastinki peremennoy tolschiny*. Moscow: Fizmatgiz, 294.
7. Babakov, I. M. (2004). *Teoriya kolebaniy*. Moscow: Drofa, 591.
8. Trapezon, K. A. (2012). Method of symmetries at the vibrations of circular plates of variable thickness. *Electronics and Communications*, 6, 66–77. doi: <https://doi.org/10.20535/2312-1807.2012.17.6.11401>
9. Golmakani, M. E., Emami, M. (2016). Buckling and large deflection behaviors of radially functionally graded ring-stiffened circular plates with various boundary conditions. *Applied Mathematics and Mechanics*, 37 (9), 1131–1152. doi: <https://doi.org/10.1007/s10483-016-2122-6>
10. Chen, H., Wu, R., Xie, L., Du, J., Yi, L., Huang, B. et. al. (2020). High-frequency vibrations of circular and annular plates with the Mindlin plate theory. *Archive of Applied Mechanics*, 90 (5), 1025–1038. doi: <https://doi.org/10.1007/s00419-019-01654-6>
11. Ukrainskii, D. V. (2018). On the Type of Flexural Edge Wave on a Circular Plate. *Mechanics of Solids*, 53 (5), 501–509. doi: <https://doi.org/10.3103/s0025654418080046>
12. Zhang, J. H., Liu, X., Zhao, X. (2019). Symplectic Method-Based Analysis of Axisymmetric Dynamic Thermal Buckling of Functionally Graded Circular Plates. *Mechanics of Composite Materials*, 55 (4), 455–466. doi: <https://doi.org/10.1007/s11029-019-09825-w>
13. Van Do, V. N., Lee, C.-H. (2018). Nonlinear thermal buckling analyses of functionally graded circular plates using higher-order shear deformation theory with a new transverse shear function and an enhanced mesh-free method. *Acta Mechanica*, 229 (9), 3787–3811. doi: <https://doi.org/10.1007/s00707-018-2190-7>
14. Yang, Y., Zhang, Y., Chen, W., Yang, B. (2018). On asymmetric bending of functionally graded solid circular plates. *Applied Mathematics and Mechanics*, 39 (6), 767–782. doi: <https://doi.org/10.1007/s10483-018-2337-7>
15. Yuan, J., Chen, W. (2017). Exact solutions for axisymmetric flexural free vibrations of inhomogeneous circular Mindlin plates with variable thickness. *Applied Mathematics and Mechanics*, 38 (4), 505–526. doi: <https://doi.org/10.1007/s10483-017-2187-6>
16. Trapezon, K. A. (2006). The symmetry method in calculating and designing of acoustic thickeners. *Akusticheskiy vestnik*, 9 (4), 50–55.
17. Tymoshenko, S., Voiniv'skiy-Kriher, S. (1959). *Theory of Plates and Shells*. New York: McGraw-Hill, 416.
18. Trapezon, K. A. (2015). Variant of method of symmetries in a task about the vibrations of circular plate with a decreasing thickness by law of concave parabola. *Electronics and Communications*, 20 (2 (85)), 90–99. doi: <https://doi.org/10.20535/2312-1807.2015.20.2.47781>
19. Kornilov, A. A. (1968). Kolebaniya kol'tsevoy plastiny peremennoy tolschiny proizvol'nogo profilya s uchetom inertsii vrascheniya i deformatsii sdviga. *Vestnik KPI. Seriya: Mashinostroenie*, 8, 62–68.
20. Trapezon, A. G. (1983). Raschet uprugih elementov pri rezonansnyh ustalostnyh ispytaniyah. *Kyiv: Naukova dumka*, 96.